Biointerface Research in Applied Chemistry
Platinum Open Access Journal (ISSN: 2069-5837)

Article
Volume 12, Issue 6, 2022, 8307 - 8323
https://doi.org/10.33263/BRIAC126.83078323

Flavonoids in Benign Prostate Hypertrophy: Identification in Herbal Preparations and Molecular Docking Approach

Huda Mando [1,*], Ahmad Hassan [1], Nathalie Moussa [2]

[1] Department of Pharmaceutical Chemistry and Quality Control of Medicaments, Faculty of Pharmacy, Damascus University, Damascus, Syria; hodamandomando@hotmail.com (H.M.), aha226@gmail.com (A.H.);
[2] Department of Pharmaceutical Chemistry and Quality Control of Medicaments, Faculty of Pharmacy, Al andalus University for medical science, Tartus, Syria; n.mousa@au.edu.sy (N.M.);
* Correspondence: hodamandomando@hotmail.com (H.M.);

Scopus Author ID 55255180500

Received: 20.10.2021; Revised: 24.11.2021; Accepted: 27.11.2021; Published: 10.12.2021

Abstract: The benefits of phytotherapy in Benign prostatic hyperplasia (BPH) are of interest where they may lack side effects at long-term therapy. Through plant-derived preparations are *Saw palmetto* and Pumpkin seed oil. Evidence suggests that fatty acids, phytosterols, tocopherols, and flavonoids are the active components responsible for alleviating BPH symptoms. Flavonoids are reported to inhibit BPH through different mechanisms. Reducing inflammation and lowering reactive oxygen species are amongst the proposed mechanisms. *In vitro* studies highlighted the role of flavonoids in 5-alpha reductase II (5ARII) inhibitory activity. In this study, herbal preparations known to treat BPH were subjected to LC/MS/MS analysis integrated with multiple reaction monitoring (MRM) to identify the content of flavonoids. A molecular docking study was conducted on the assigned flavonoids to predict the binding mode and interaction with the targeted 3D- crystal structure of the human 5ARII enzyme. Results showed the existence of seven flavonoids and a polyphenol compound. Sakuranetin, Isorhamnetin, and Chlorogenic acid were not reported before. Molecular docking outcomes revealed that Astragalin, Isoquercitrin, Quercetin, and Chlorogenic acid have similar binding affinity to the reference Finasteride compound. These findings suggest flavonoids as potent potential inhibitors of 5ARII and could proceed to *in vitro* investigations.

Keywords: BPH; herbal preparations; *Saw palmetto*; flavonoids; LC-MS-MS; molecular docking.

1. Introduction

Benign prostatic hyperplasia (BPH) is one of the most common geriatric male disorders worldwide, increasing prevalence [1]. The rate of incidence increases notably in aging males, with a progressive augment in prevalence to nearly 80% in men over 80 years of age [2]. Enlargement of prostate and boost in cell number is due to the stromal and epithelial proliferation and/or to impaired programmed cell death or apoptosis resulting in cellular accumulation. Androgens, growth factors, and neurotransmitters may participate either solely or in combination in the etiology of the hypertrophic process [3]. Treatment options of BPH are largely based on two classes of medications; alpha one-adrenergic antagonists (α1AA) and 5-alpha reductase II inhibitors (5ARIIs) [4]. Being potent anti-inflammatory drugs, phosphodiesterase inhibitors provide additional options to treat prostatic inflammation [5]. FDA approved in October 2011 the usage of tadalafil for treatment of BPH. Combining an alpha-blocker and 5ARIIs may slightly ameliorate urinary symptoms [6]. Combination therapy

between alpha one-adrenergic antagonists and 5ARII inhibitors is the gold benchmark for BPH remedy even though accompanied by significantly higher rates of erectile dysfunction(ED) and libido alterations (LA) [7]. Recently, the medical management of BPH has been largely based on phytotherapy. Blood pressure and sexual function are the main drawbacks of conventional therapies, mainly α1AA and 5ARII inhibitors. Plant-derived preparations fill the need for treatment with fewer reverse effects [8]. Versatile plants are available for the handling of BPH with different mechanisms. Inhibition of 5ARII is one of the proposed mechanisms through which certain active components play a role in the mechanism of inhibition. Herbal remedies in the literature proved to benefit BPH by inhibition of 5AR include *Alpinia officinarum, Brassica napus, Camellia sinensis, cucurbita seed oil, Lygodium japonicum, Pinus sp, Polygonum multiflorum Thunb, Rosa multiflora,* and *Serenoa repens*. Animal studies revealed that Steroidal compounds, Lauric and myristic acids, stearic, oleic, palmitic and linoleic acids, daidzin, polyphenolic compounds, and Isoflavones alleviate symptoms by different mechanisms involving 5ARII inhibitory activity, anti-androgen activity, anti-proliferative activity, and anti-inflammatory activity [9]. No evident side effects were observed in human studies of *P. africanum* alone or in combination with stinging nettle extracts and proved to be effective in comparison with placebo. In one trial that lasted for 12 months, *S. repens* proved to be equal to tamsulosin in the medical treatment of symptoms accompanied with BPH [10]. Tolerability was significant and effectiveness similar to finasteride during 24 weeks of treatment with *Serenoa repens* and *Urtica dioica* [11].

Saw palmetto is the third best-selling plant as a food supplement in America [12]. There are more than 30 types of plants used to treat BPH. More than half of the formulations contained the dry fruit extract of Serenoa repens, while the remainder contained *Prunus africana*, rye pollen extract, betasitosterol, stinging nettle (*Urtica dioica*), and Cucurbita pepo [13,14]. In silico studies brought phytosterols, fatty acids, and tocopherols as potential inhibitors to 5ARII [15-17]. Efficacy and safety of polyphenol treatment in the prevention and treatment of BPH *in vivo* and *in vitro* have been reported in recent years [18]. *In vitro* studies bring-to-light Naringenin, Luteolin, Kaempferol [19,20], and Isoflavones [21] as active herbal components in several plant preparations used to relieve BPH symptoms. The whole-cell assay proved daidzein, genistein, and kaempferol to be better inhibitors of the type II isozyme than the type 1 [22].

Astragalin, the glycoside form of kaempferol, is known for its diverse therapeutic properties such as antioxidant, anti-inflammatory, and antiviral [23,24].

Quercetin-3-O-neohesperidoside and Rutin are the main components of multiple herbal preparations with anti-inflammatory effects [25]. *In vitro, in vivo,* and *in silico* studies brought Quercetin as a potent inhibitor of SARS-CoV 2 by preventing the entry of the virus in the host cell, binding the S protein, and inhibiting ACE2 receptors [23].

Isorhamnetin is an active ingredient in many plants mainly contained in *Hippophae rhamnoides* and *Ginkgo biloba*, with numerous effects on cardiovascular and cerebrovascular protection, anti-tumor, anti-inflammatory, and anti-oxidation activity [26].

In this study, herbal preparation containing *Saw palmetto* (figure 1) from retail pharmacies was assessed by identifying flavonoids via LC/MS/MS method. Molecular docking simulation of flavonoids and polyphenols identified in the studied herbal preparations was carried out on the crystal structure of 5ARII. A better understanding of binding mode and interactions will add insight to their potential application in BPH control. While previous molecular modeling studies of diverse structures were made on homology models [27], a 3D

X-ray crystal structure of 5ARII has been deposited in a protein data bank recently [28]. Screening the herbal preparations for the content of flavonoids and studying the interactions with the targeted protein by molecular docking approach will support and strengthen the theories and studies that correlate the activity of herbal formulations to certain components. To our knowledge, this is the first study of molecular docking of flavonoids performed on the human 3D X-ray crystal structure of 5ARII.

Figure 1. *Saw palmetto.*

2. Materials and Methods

2.1. Identification of flavonoids.

2.1.1. Reagents and samples.

Solvents were of LC/MS grade (Merck).Sawbal® tablets and Mivolis® capsules were supplied from a retail pharmacy.

2.1.2. Sample preparation.

Twenty tablets of Sawbal® were crushed, and twenty capsules of Mivolis® were opened and emptied. One gram of each content was dissolved in 10 mL methanol and sonicated for 2 h. The methanol layer was taken and passed through a 0.22 µm filter and injected directly to LC-MS-MS.

2.1.3. LC-ESI-MS analysis.

Agilent LC-MS-MS system (USA) liquid chromatography (*Triple Quadrupole 6420*) with electrospray ionization (ESI) equipped with mass spectrometry was used for the identification of flavonoids. The column was Eclipse XDB C18, 4.6 * 150 mm, 3.5µm. The mobile gradient phase consisted of a mixture of (A) water acidified with 0.1% formic acid (B) acetonitrile. Gradient elution was applied as indicated: 15%-20% B for 0-5 min, 20%-28% B for 5-6 min, 28% B for 6-10 minutes, 28%-35% B for 10-12 minutes, 35% B for 12-15 minutes. The flow rate was 0.6 ml/min, maintaining the temperature at 35°C. The detection was carried out in the negative ion mode by a full scan range within 100 to 2000 m/z.

2.1.4. Molecular docking of flavonoids.

The molecular docking of flavonoids was performed using the Schrodinger suite of software (Maestro, version 121) with its scores and calculations. Molecular docking in the active site of the X-ray crystal structure of 5ARII went through the following steps [29].

2.1.5. Ligand preparation.

The 2D structures of the studied compounds were downloaded as standard structure-data file (SDF) format using the world's largest collection of freely accessible chemical information PubChem [30]. After that, they were converted into the protein data bank (PDB) format using the freely abundant open-source toolbox, Open Babel 3-1-1 [31]. The energy was minimized using potential liquid simulations (OPLS3) force field in Lig Prep in Maestro version 12.1 (Schrödinger, LCC, New York, 2019) [32,33]. The three-dimensional (3D) conformer generated for each ligand with the lowest energy was used during the docking procedure.

2.1.6. Protein preparation.

The 3D structure of 5ARII (PDB code: 7BW1, 2.8 Å) was retrieved from PDB and prepared. Water molecules and co-crystallized ligands were removed. Explicit hydrogen atoms were added. Bond orders and formal charges were adjusted, while disulfide bonds were created, and overlaps were checked. The corrected structure was subjected to energy minimization to relax any strain caused by the adjustment. The last step was preceded by repairing important protein errors such as incomplete residues [34].

2.1.7. Grid generation.

This step was obtained by Schrödinger in order to create a rigid network around the residues that form the functional binding groups at the binding site within the protein. The default box size is 20 angstroms and is centered on the default ligand.

Grids for molecular docking with Glide16 were calculated with a hydrogen bond constraint to glutamic acid 57 of 5ARII [35].

2.1.8. Extra precision (XP) molecular docking.

An extra precision (XP) glide docking was used to perform the docking and to predict the binding mode between the identified flavonoids and 5ARII. Compounds were flexibly docked with glide within the rigid binding site [36]. One docking hit with the least glide docking score indicating the most favorable pose is obtained for each ligand to be analyzed later [37]. Finally, the results were rendered in the work table as a pose viewer file.

3. Results and Discussion

3.1. Identification of flavonoids.

Acetonitrile was chosen as the organic phase due to its higher sensitivity and lower background than methanol. As for formic acid, it was added at a rate of 0.1% to the mobile phase, and it is facilitated better resolution by reducing peak tailing [38]. The negative ionization mode [M-H]- was chosen because it gives an extensive MS-MS fragmentation compared to [M+H]+ [39]. Flavonoids were recognized by LC-MS-MS data and information available in the literature, with subsequent confirmation by multiple reaction monitoring (MRM). This recognition provided by MS/MS has enormous advantages in reducing interference and enhancing sensitivity compared to single-SIM modulation [40]. MRM scan

mode is the best way to restrain the accuracy with specific ion fragmentation from the precursor ion to its specific fragmentation ion (by daughter ion) [39].

In the MS-MS spectrum, the loss of glycosyl moieties in the positive and negative ionization modes, as well as the molecular fragments, is observed due to the retro Diels–Alder (RDA) [41] fragmentation pathway, which implies dissociation of the glycosides to their original components.

The chromatogram obtained by LC-MS-MS of Sawbal methanolic extract showed eight peaks in the full scan mode represented by Figure 1.

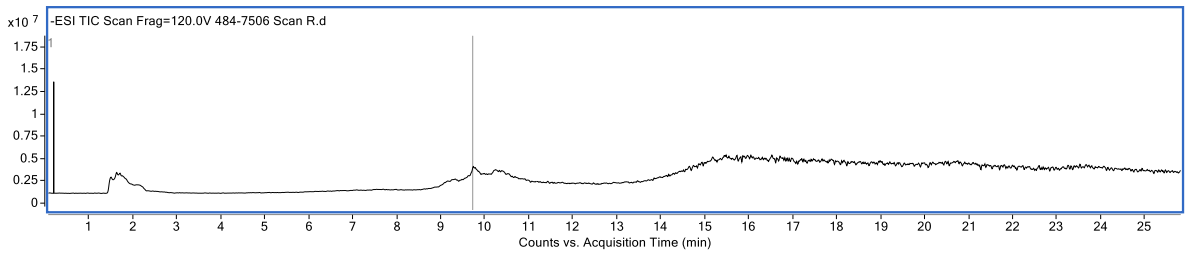

Figure 2. Chromatogram of Sawbal methanolic extract in the full scan mode.

Eight flavonoids were initially identified in the methanolic extract by mass, fragmentation mass spectrometry (molecular masses of potential components), and information available in the literature (Table 1). Most of the compounds identified gave the deprotonated molecule [M−H]- representing the predominant precursor ions except for Quercetin 3-O-neohesperidoside, which gave the parent fragment without deprotonation, and Rosmarinic acid, which gave the fragment 357.2 which is [M-H-2H]-

Peak 1 (1.617) with a [M−H]- ion m/z 447 and daughter ion at m/z 285 was identified as Astragaline. The daughter ion m/z 285 represents the fragment belonging to the kaempferol glycoside after cleavage of the glycoside molecule, as in Fig 2, [42].

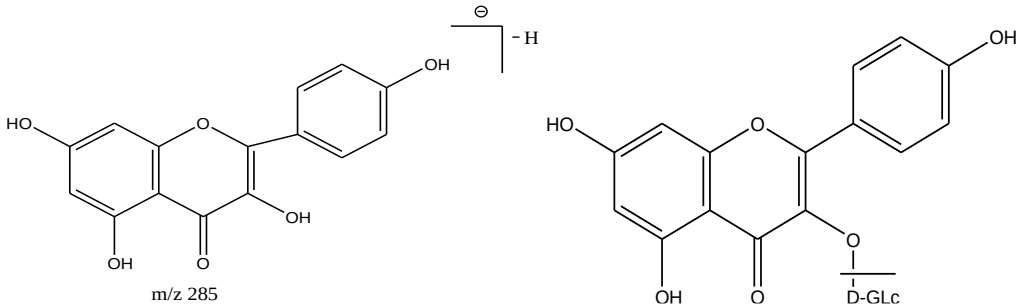

Figure 3. (a) Astragaline structure (b) ion m/z 285.

Peak 2 (1.628) with the fragment 610 Da and daughter ion at m/z 179 was identified as Quercetin 3-O-neohesperidoside, as can be seen in Figure 3, [43].

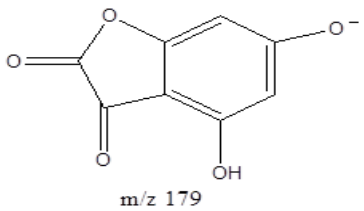

Figure 4. Fragment m/z 179 of Quercetin.

Peak 3 (1.650) with a [M−H]−ion m/z 316.9 and daughter ion at m/z 179 was identified as Myricetin [44] in Figure 4.

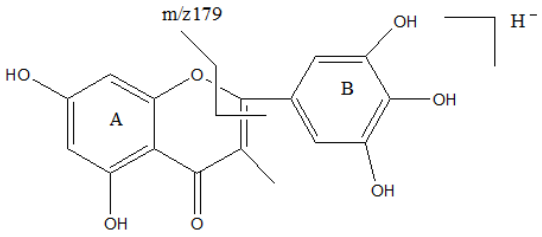

Figure 5. Fragment m/z 179 of Myricetin.

Isorhamentin at 2.116 was identified by the molecular ion m/z 316.9 and daughter ion 272.8, as shown in Figure 5 [45,46].

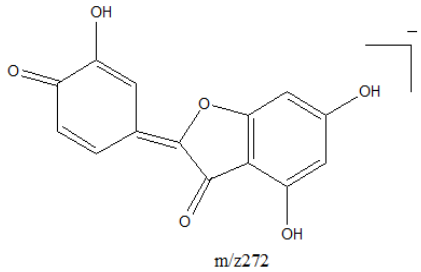

Figure 6. Fragment m/z 272 of Isorhamentin.

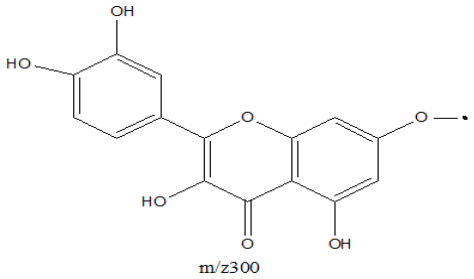

Figure 7. Fragment m/z 300 of Rutin.

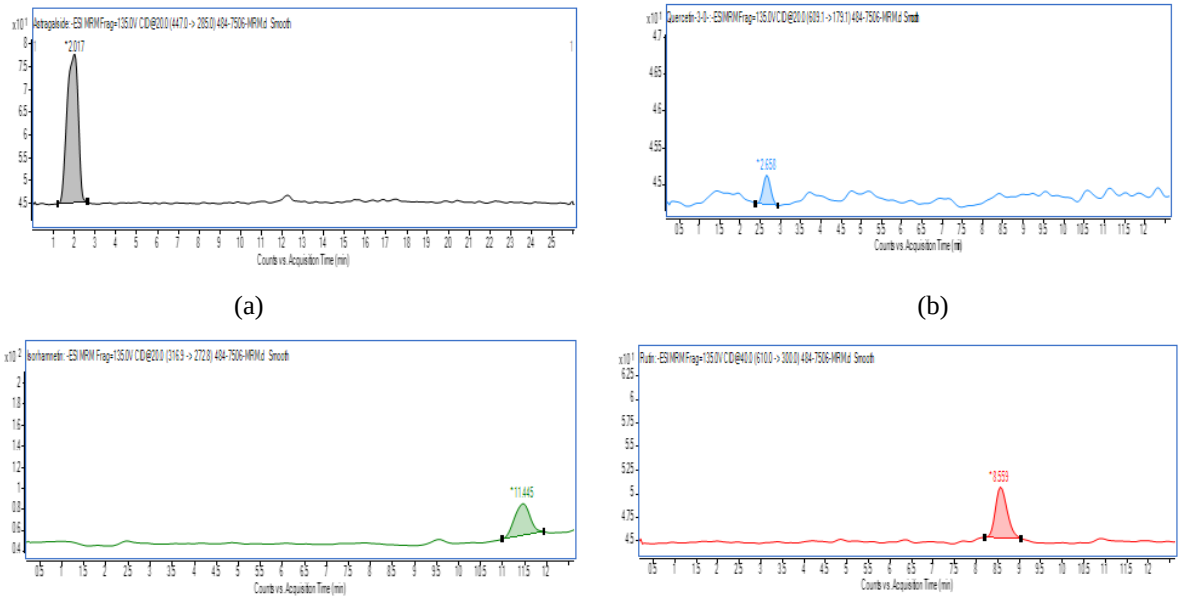

(a) (b)

(c) (d)

Figure 8. Chromatogram of flavonoids identified by MRM in methanolic extract of Sawbal®: (a) Astragaline; (b) Quercetin-3-O-neohesperidoside; (c) Isorhamnetin; (d) Rutin.

Table 1. The flavonoids identified in methanolic extract of Sawbal® by LC-MS-MS.

	Compound	Structure	Retention time (min)	Fragments (m/z)
Sawbal®	Astragaline C21H20O11 5,7-dihydroxy-2-(4-hydroxyphenyl)-3-[(2S,3R,4S,5S,6R)-3,4,5-trihydroxy-6-(hydroxymethyl)oxan-2-yl]oxychromen-4-one	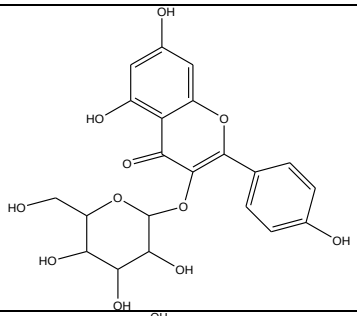	1.617	447.2 m/z > 226.9 m/z
	Quercetin 3-Oneohesperidoside C27H30O16 3-[(2S,3R,4S,5R,6R)-4,5-dihydroxy-6-(hydroxymethyl)-3-[(2S,3R,4R,5R,6S)-3,4,5-trihydroxy-6-methyloxan-2-yl]oxyoxan-2-yl]oxy-2-(3,4-dihydroxyphenyl)-5,7-dihydroxychromen-4-one	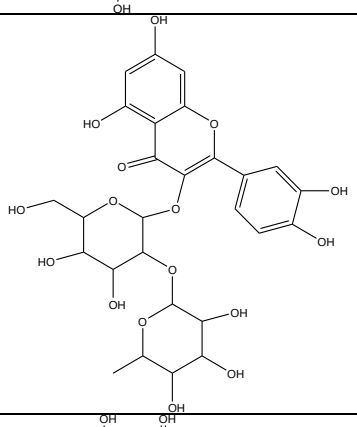	1.628	610.4 m/z > 179.1 m/z
	Myricetin C15H10O8 3,5,7-trihydroxy-2-(3,4,5-trihydroxyphenyl)chromen-4-one	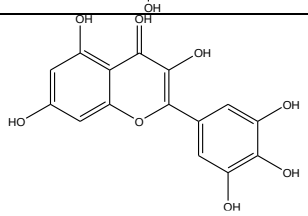	1.650	316.9 m/z > 179 m/z
	Rosmarinic acid C18H16O8 (2R)-3-(3,4-dihydroxyphenyl)-2-[(E)-3-(3,4-dihydroxyphenyl)prop-2-enoyl]oxypropanoic acid	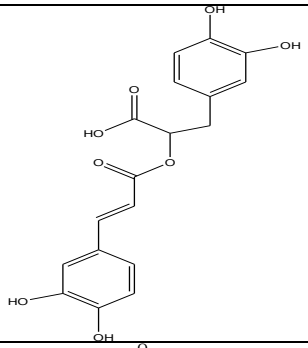	1.997	357.2 m/z > 161.1 m/z
	Isorhamentin C16H12O7 3,5,7-trihydroxy-2-(4-hydroxy-3-methoxyphenyl)chromen-4-one	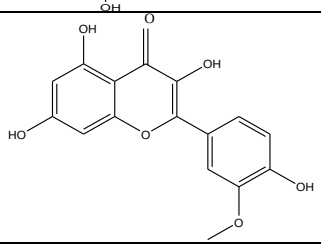	2.116	316.9 m/z > 272.8 m/z
	Catchin C15H14O6 (2R,3S)-2-(3,4-dihydroxyphenyl)-3,4-dihydro-2H-chromene-3,5,7-triol	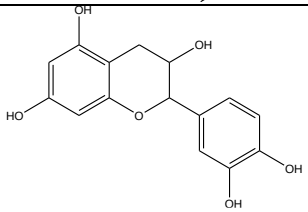	9.725	847 m/z>265 m/z

	Compound	Structure	Retention time (min)	Fragments (m/z)
	Rutin C27H30O16 2-(3,4-dihydroxyphenyl)-5,7-dihydroxy-3-[(2S,3R,4S,5S,6R)-3,4,5-trihydroxy-6-[[(2R,3R,4R,5R,6S)-3,4,5-trihydroxy-6-methyloxan-2-yl]oxymethyl]oxan-2-yl]oxychromen-4-one	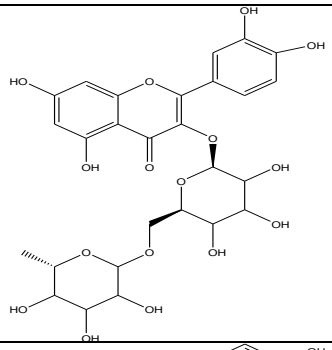	10.333	610 m/z > 255 m/z
	Kaempferol-3-O-(2G-α-L-rhamnosyl)-rutinosid C33H40O19 3-[6-[[4,5-dihydroxy-6-methyl-3-(3,4,5-trihydroxy-6-methyloxan-2-yl)oxyoxan-2-yl]oxymethyl]-3,4,5-trihydroxyoxan-2-yl]oxy-5,7-dihydroxy-2-(4-hydroxyphenyl)chromen-4-one	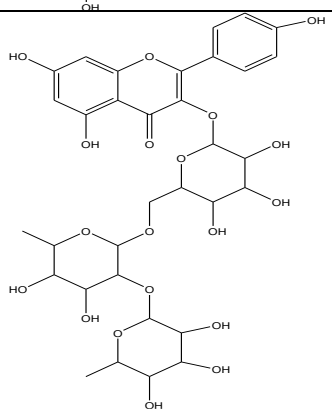	10.333	740 m/z > 255 m/z

Peaks 4, 6, 7, and 8 were identified as Rosmarinic acid (1.997) [47], catchin (9.725) [45], Rutin (10.33) [46] (Figure 6), Kaempferol-3-O-(2G-α-L-rhamnosyl)-rutinosid (10.33) respectively by their molecular and daughter ions (Table 1).

After initiative identification of flavonoids in Sawbal®, MRM was applied to confirm the presence of the initially assigned ones. During MRM analysis, certain daughter ions are selected through the second quadrupole, transitioning from the molecular ion-specific to its production. 447 > 285 m/z, 316.9 > 272.8 m/z, 610.4 m/z > 179.1 m/z, 610 > 300 m/z were chosen as the qualifier ion transition of Astragaline, Isorhamnetin, Quercetin-3-O-neohesperidoside, and Rutin respectively. Figure 7, Shows the chromatograms of the identified flavonoids in methanolic extract of Sawbal® by LC-MS-MS/ MRM mode.

The chromatogram obtained by LC-MS-MS of Mivolis® methanolic extract in the full scan mode is represented in Figure 8.

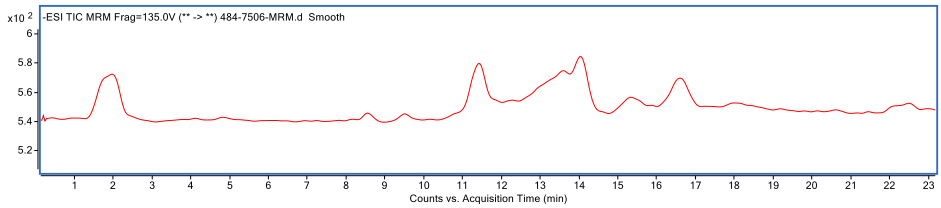

Figure 9. Chromatogram of Mivolis® methanolic extract in the full scan mode.

Chlorogenic acid and 7 flavonoids are identified in Mivolis® methanolic extract by LC-MS-MS- MRM. The presence of chlorogenic acid is confirmed by the precursor ion m/z 353 and daughter ion m/z 191 expressing quinic acid (Fig 10), [48].

The presence of a Sakuranetindimer polymer is also confirmed by the molecular fragment m/z 551, which results from the meeting of two Sakuranetin molecules and the exit of a water molecule and H2 and the daughter fragment m/z 197. Previous studies have shown

the existence of carbon-carbon bonds between a flavonoid and another, such as Sakuranetin 3,8 homodimer and Chamaejasmin [49].

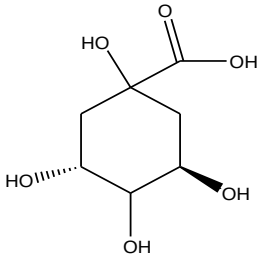

Figure 10. Fragment m/z 191 of quinic acid.

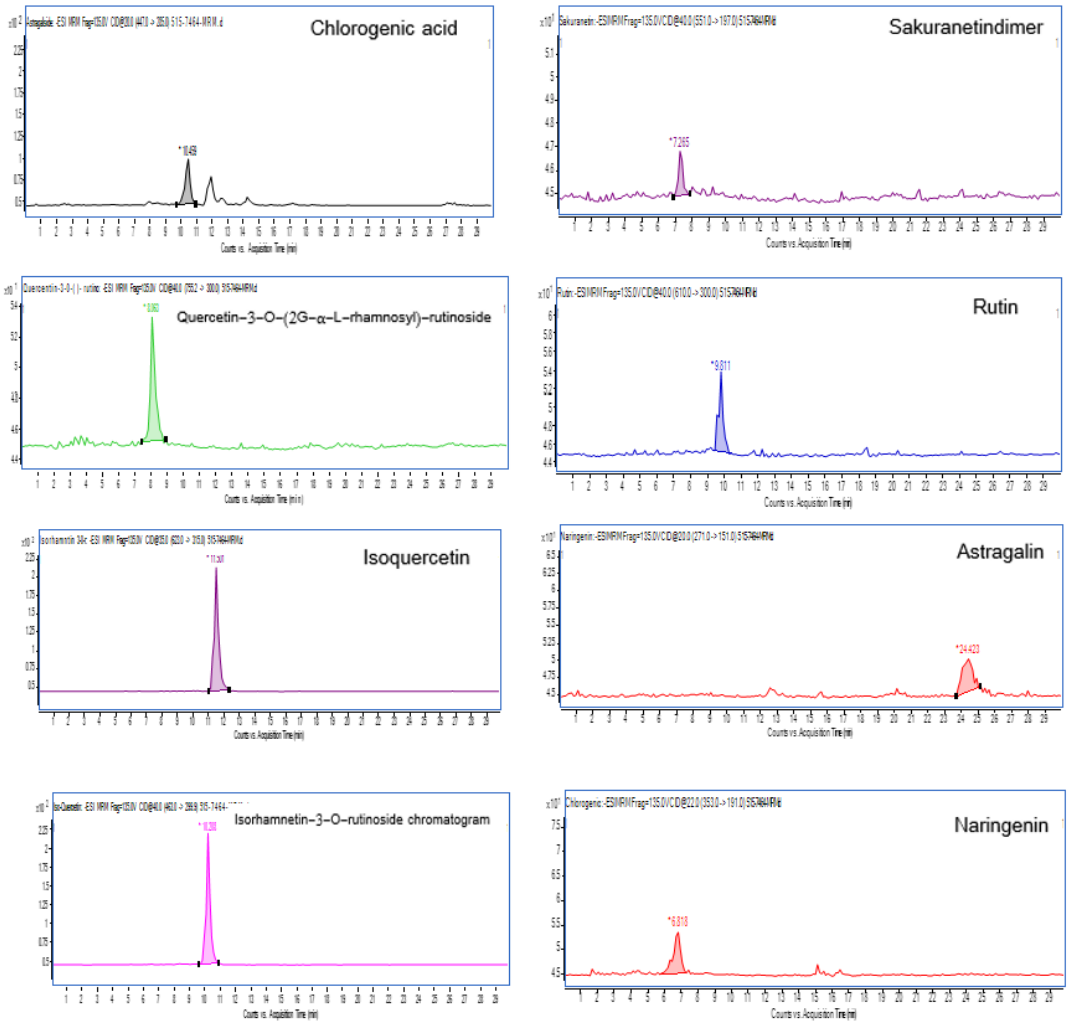

Figure 11. Chromatogram of Chlorogenic acid and flavonoids identified by MRM in methanolic extract of Mivolis®.

Quercetin-3-O-(2G-α-L-rhamnosyl)-rutinoside is defined based on precursor fragment m/z 755.2 and daughter fragment m/z 300 [46]. Similarly, the compound Rutin is defined based on the molecular ion m/z 610 and the daughter fragment m/z 300, and according to a recent study, this compound inhibits the protease enzyme of SARS-CoV-2 [50].

Figure 11 depicts the chromatogram of Chlorogenic acid and flavonoids identified by MRM in methanolic extract of Mivolis®.

Isoquercetin, Astragalin, Isorhamnetin-3-O-rutinoside, and Naringenin are identified by the ions m/z 463.0/299.9 [51], 447.0/285 [43] and 623/315 [52], 272/151 [53,54]

respectively. The fragmentation pattern of Isorhamnetin-3-O-rutinoside is shown in Figure 12. The product ion m/z 151 in Naringenin is illustrated in Figure 13.

Astragalin inhibits SARS-CoV-2, according to a recent study [24], in addition to its anti-inflammatory activity. The flavonone Naringenin is present in many vegetables and fruits and has strong antioxidant, antiviral and anti-inflammatory, properties [55-57]. Its beneficial effect against SARS-CoV-2 is exerted by inhibiting the main protease and reducing ACE2 activity [24]. The identified active components of Mivolis® are listed in Table 2.

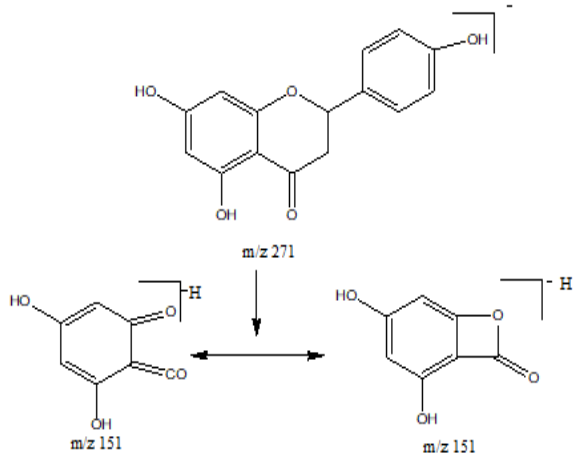

Figure 13. Interpretation of the fragment m/z 151 in Naringenin.

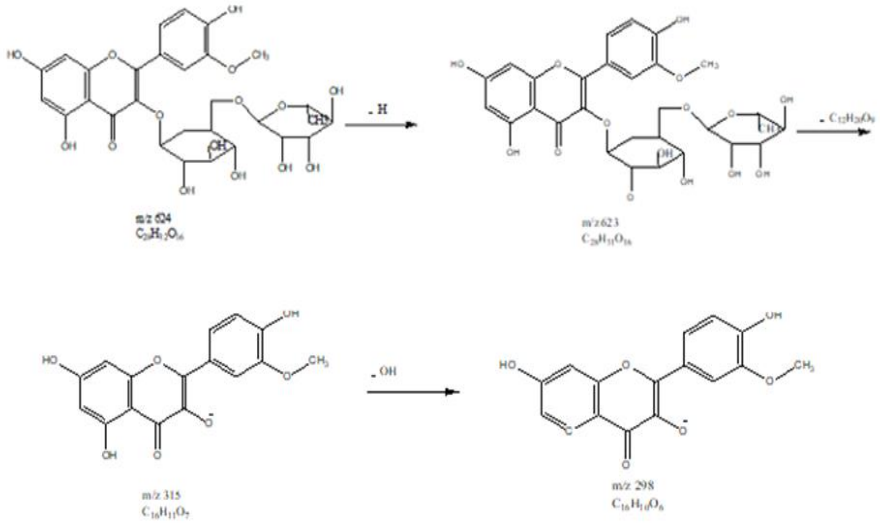

Figure 12. Interpretation of the fragments of Isorhamnetin-3-O-rutinoside.

Table 2. The flavonoids identified in methanolic extract of Mivolis® by LC-MS-MS/MRM mode.

Compound	Structure	MW	Molecular formula	Fragments m/z
Chlorogenic acid C16H18O9 (1S,3R,4R,5R)-3-[(E)-3-(3,4-dihydroxyphenyl)prop-2-enoyl]oxy-1,4,5-trihydroxycyclohexane-1-carboxylic acid	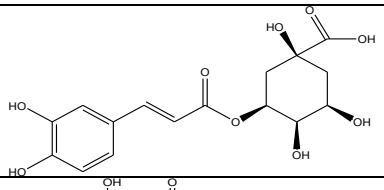	354.31	C16H18O9	353 > 191
Sakuranetin C16H14O5 (2S)-5-hydroxy-2-(4-hydroxyphenyl)-7-methoxy-2,3-dihydrochromen-4-one	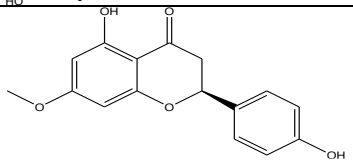	286.26	C16H14O5	551> 197

Quercetin-3-O-(2G-α-L-rhamnosyl)-rutinoside C33H40O20	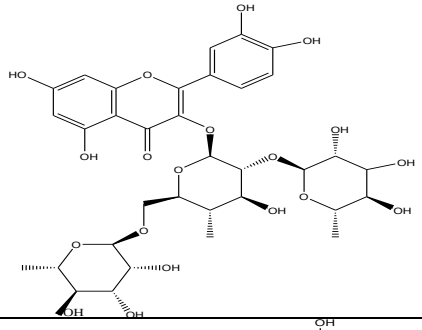	756.65	C33H40O20	755.2 >300
Rutin C27H30O16 2-(3,4-dihydroxyphenyl)-5,7-dihydroxy-3-[(2S,3R,4S,5S,6R)-3,4,5-trihydroxy-6-[[(2R,3R,4R,5R,6S)-3,4,5-trihydroxy-6-methyloxan-2-yl]oxymethyl]oxan-2-yl]oxychromen-4-one	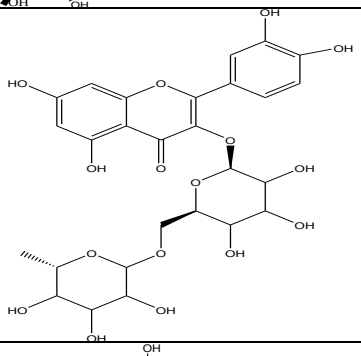	610	C27H30O16	610 > 300
Isoquercetin C21H20O12 2-(3,4-dihydroxyphenyl)-5,7-dihydroxy-3-[(2S,3R,4S,5S,6R)-3,4,5-trihydroxy-6-(hydroxymethyl)oxan-2-yl]oxychromen-4-one	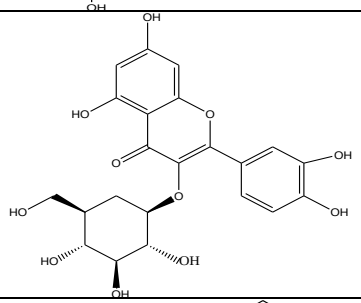	464.4	C21H20O12	436 >299.9
Astragaline C21H20O11 5,7-dihydroxy-2-(4-hydroxyphenyl)-3-[(2S,3R,4S,5S,6R)-3,4,5-trihydroxy-6-(hydroxymethyl)oxan-2-yl]oxychromen-4-one	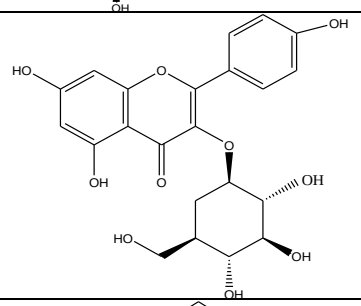	448	C21H20O11	447 > 285
Isorhamnetin-3-O-rutinoside C28H32O16 5,7-dihydroxy-2-(4-hydroxy-3-methoxyphenyl)-3-[(2S,3R,4S,5S,6R)-3,4,5-trihydroxy-6-[[(2R,3R,4R,5R,6S)-3,4,5-trihydroxy-6-methyloxan-2-yl]oxymethyl]oxan-2-yl]oxychromen-4-one	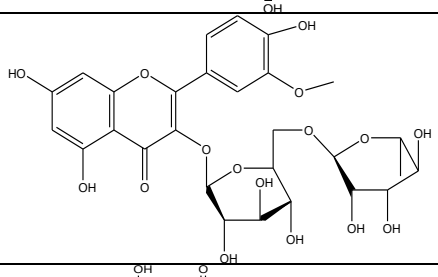	624.13	C28H32O16	623 > 315
Naringenin C15H12O5 5,7-dihydroxy-2-(4-hydroxyphenyl)-2,3-dihydrochromen-4-one	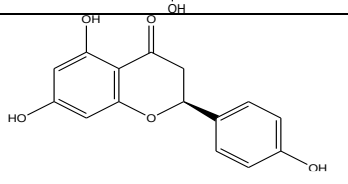	272	C15H12O5	272 > 151

Table 3. Types of interactions between the flavonoids and the binding site of 5ARII.

	Charged -	**Charged +**	**hydrophobic**	**Polar**	**H-bond**	**pi-pi**	**Glide /score**
Finasteride	Glu57		TYR91,33,107.	Gln56,Ser31	Glu57		-8.79
			PHE223,219,118.ALA		Arg114		
			24,		TYR91		
			LEU224,111,23,20.C				
			YS119.TRP53.VAL27				
Chlorogenic	ASP164,	ARG171,	TYR178,98,33.LEU16	ASN193,160	ARG171,	TRP53	-8.779
acid	GLU197	105,227,9	7,224,TRP53PHE194,	.HIE231	227.TYR1		

	Charged -	Charged +	hydrophobic	Polar	H-bond	pi-pi	Glide /score
		4.LYS35.			78.ASP16		
					4,ASN160		
					,197,HIE2		
					31		
Astragaline	GLU57,19	ARG94,2	TYR91,107,33.PHE19	SER31,220.	SER220.	PHE216,	-8.225
	7	27,114	4,216,219,223,218.LE	ASN160.GL	GLU57.A	219	
			U111,224.TRP53,201	N56	RG94		
Isoquercetin	GLU57,19	ARG94,2	LEU167,PHE186,	SER31,220.	ASN193		-7.679
	7,ASP164	27,114.H	ALA192.PHE234	ASN160,GL	GLY191		
		P90		N56	SER190		
Quercetin-	GLU197,5	ARG114,	PHE194,223,118,119,	SER31,220.	TYR91,98	PHE33,2	-7.619
3-O-	7,ASP164	227,94.H	216.LEU224,167,111.	ASN193,160	,33.GLU5	23,118	
neohesperid		P90.	TYR91,98,107.TRP53	.GLN56.AG	7.ARG94		
oside			.CYS119.	N122.HE23			
Rutin	GLu57,19	ARG227,	LEU20,224,111,167.T	SER31,220.	GLU57.A	PHE194.	-6.777
	7.ASP164	94,90	YR98,107,91,33.PHE	ASN193,160	SP164.TY	ARG94	
			118,223,216,219,194.	.GLN56	R91,33.S		
			TRP53,201.CYS119		ER31		
Isorhamnitin	GLu57,19	ARG94,1	PHE216,194,223,219,	SER31.ASN	TYR91.A	ARG94.	-6.762
	7	14.HIP90	118.LEU224,111,TYR	160.GLN56.	RG94.GL	TRP53	
			91,33,107.TRP201,53		U197		
			.CYS119				
Sakuranetin	GLU197,5	ARG94.HI	PHE194,223,118,219,	ASN160,193	GLU197.T	ARG94	-6.729
	7	P90	216.TYR107,33,91.T	.GLN56	YR91.LE		
			RP53,201.CYS119.LE		U111		
			U224,111				
Isorhamnetin	GLu197,5	ARG94,1	PHE216,223,194,219,	ASN160.GL	GLU197.	TRP53.A	-6.300
-3-O-	7	14.HIP90	118.TRP201,53.TYR9	N56.SER31	ARG94.T	RG94	
rutinoside			1,33,107.LEU111,224		YR91.		
			.CYS119				
Naringenin	GLU57,19	HIP90.AR	TYR98,91,33.PHE216	ASN160,193	TYR91.A	PHE118	-6.109
	7.ASP164	G94	,223,118,194.LEU224		SP164.AS		
			.TRP53.CYS119		N160		

3.2. Molecular docking of flavonoids.

Root mean square deviation (RMSD) between the crystal ligand and re-docked ligand (finasteride) was less than the X-RAY resolution (1.5), revealing acceptable harmony between the experimental and predicted binding pose [58].

The extra precision glide docking scores for the identified flavonoids ranged between -6.109 and -8.779. The score of finasteride as a potent reference 5ARII was -8.79. Chlorogenic acid and Astragalin fit well in the 5ARII binding site with a glide score close to finasteride (Figures 13, 14, and 15). Astragalin, Quercetin-3-O-neohesperidoside, and Rutin can create a hydrogen bond with GLU57 as finasteride do, where Quercetin-3-O-neohesperidoside, Rutin, Isorhamnitin, Sakuranetin, Isorhamnetin-3-O-rutinoside, and Naringenin can bind to TYR91 with a hydrogen bond as in finasteride (Table 3). None of the compounds bonded with ARG114 as finasteride. All the compounds participated in pi –pi attacking (except Isoquercetin) by their TRP and PHE residues. ARG94 was involved in pi-pi stacking in Rutin, Isorhamentin, Sakuranetin, and Isorhamnetin-3-O-rutinoside. Although π- π stacking is particularly known for aromatic rings where about 60% of aromatic rings show this interaction [59], ARG also can engage in such interaction via delocalized π-system of sp2-hybridized atoms of its guanidinium group [60]. Quercetin-3-O-neohesperidoside and Rutin bind with five hydrogen bonds where GLU57 and TYR91 are part of these bonds and finasteride. Chlorogenic acid has the lowest docking score among the identified polyphenols with hydrogen donating properties [61] and salt bridge interaction [62], suggesting stable ligand-enzyme complexes and well fit binding poses.

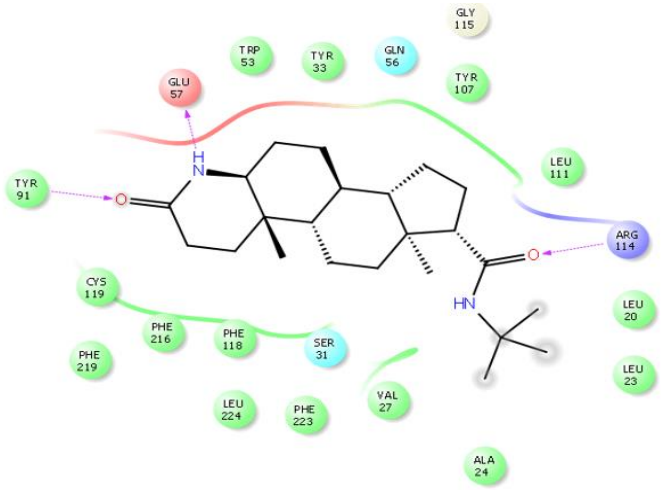

Figure 14. Schematic representation of the interactions between Dihydrofinasteride and 5ARII binding site. Hydrogen bonds with GLU57, TYR 91, and ARG114.

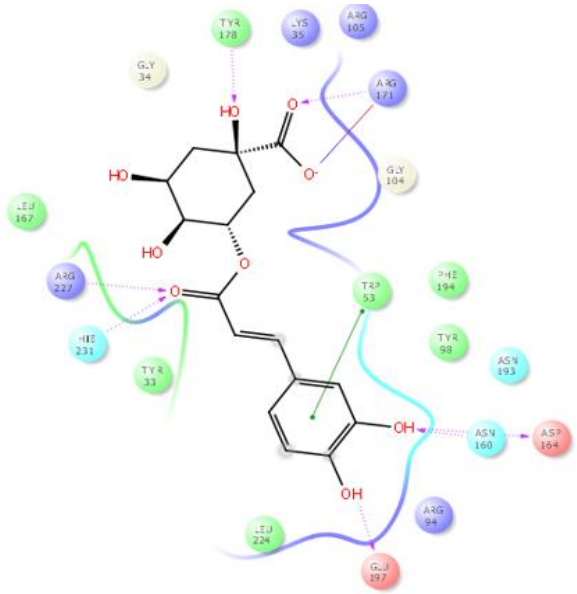

Figure 15. Schematic representation of the interactions between Chlorogenic acid and 5ARII binding site. Hydrogen bonds with TYR178, ARG171, ARG227, HIE231, GLU197, ASN160, and ASP164. Pi-pi stacking with TRP53. Salt bridge with ARG171.

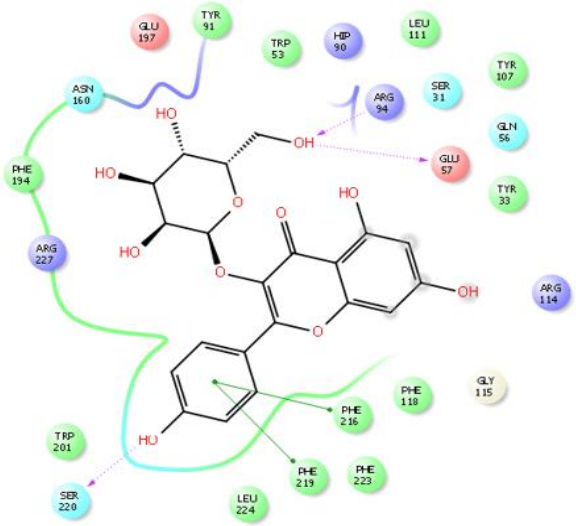

Figure 16. Schematic representation of the interactions between Astragaline and 5ARII binding site. Hydrogen bonds with ARG94, GLU57, and SER220. Pi-pi stacking with PHE216, PHE219.

4. Conclusions

Different types of inhibitors of 5ARII inhibitors were developed during the last decade. In this study, we identified flavonoids in products containing Serenoa repens. MRM mode integrated with LC-MS-MS ascertained the presence of 7 flavonoids beside Chlorogenic acid. Isorhamnitin, Sakuranetin, and Chlorogenic acid were identified with no previous reports about their presence in such botanical preparations. Identification of these compounds may enhance consumer interest, augment sales, and boost the value of their preparations. Combining Molecular docking studies with other *in vitro* and *in vivo* provides a better understanding of binding modes and enhances the hypothesis of active components' activity. Chlorogenic acid, a potent antioxidant polyphenol, exhibited high affinity towered 5ARII with7 hydrogen bonds, π- π stacking, salt bridge, and hydrophobic interactions. While salt bridges are considered the strongest inorganic interactions, they can be used to design the strongest interactions in ligand-protein complexes and thus the strongest inhibition of the enzyme. Flavonoids displayed good interactions with 5ARII implying them as potent inhibitors close to finasteride. This is the first molecular docking study on flavonoids where they appeared as potential potent inhibitors, along with Chlorogenic acid as a promising lead 5ARII inhibitor.

Funding

This research received no external funding.

Acknowledgments

This research has no acknowledgment.

Conflicts of Interest

The authors declare no conflict of interest.

References

1. Cormio, L.; Calò, B.; Falagario, U.; Iezzi, M.; Lamolinara, A.; Vitaglione, P.; Silecchia, G.; Carrieri, G.; Fogliano, V.; Iacobelli, S.; Natali, P.G.; Piantelli, M. Improvement of urinary tract symptoms and quality of life in benign prostate hyperplasia patients associated with consumption of a newly developed whole tomato-based food supplement: a phase II prospective, randomized double-blinded, placebo-controlled study. *Journal of Translational Medicine* **2021**, *19*, https://doi.org/10.1186/s12967-020-02684-3.
2. Bortnick, E.; Brown, C.; Simma-Chiang, V.; Kaplan, S.A. Modern best practice in the management of benign prostatic hyperplasia in the elderly. *Therapeutic Advances in Urology* **2020**, *12*, https://doi.org/10.1177/1756287220929486.
3. Roehrborn, C. Pathology of benign prostatic hyperplasia. *Int J Impot Res* **2008**, *20*, 11–18, https://doi.org/10.1038/ijir.2008.55.
4. DeWitt, M.E.; Gill, B.C.; Ulchaker, J.C. Cost Comparison of Benign Prostatic Hyperplasia Treatment Options. *Curr. Urol. Rep* **2019**, *20*, https://doi.org/10.1007/s11934-019-0907-3.
5. Peixoto, C.A., Gomes, F.O. The role of phosphodiesterase-5 inhibitors in prostatic inflammation: a review. *J Inflamm* **2015**, *12*, https://doi.org/10.1186/s12950-015-0099-7.
6. Pattanaik, S.; Mavuduru, R.S.; Panda, A.; Mathew, J.L.; Agarwal, M.M.; Hwang, E.C.; Lyon, J.A.; Singh, S.K.; Mandal, A.K. Phosphodiesterase inhibitors for lower urinary tract symptoms consistent with benign prostatic hyperplasia. *Cochrane Database of Systematic Reviews* **2018**, *11*, https://doi.org/10.1002/14651858.CD010060.pub2.
7. Favilla, V.; Russo, G.I.; Privitera, S.; Castelli, T.; Giardina, R.; Calogero, A.E.; Condorelli, R.A.; La Vignera, S.; Cimino, S.; Morgia, G. Impact of combination therapy 5-alpha reductase inhibitors (5-ARI) plus alpha-blockers (AB) on erectile dysfunction and decrease of libido in patients with LUTS/BPH: a systematic review with meta-analysis. *The Aging Male* **2016**, *19*, 175-181, https://doi.org/10.1080/13685538.2016.1195361.

8. Katz, A.E. Flavonoid and Botanical Approaches to Prostate Health. *The Journal of Alternative and Complementary Medicine* **2002**, *8*, 813-821, https://doi.org/10.1089/10755530260511829.
9. Azimi, H.; Khakshur, A.-A.; Aghdasi, I.; Fallah-Tafti, M.; Abdollahi, M. A Review of Animal and Human Studies for Management of Benign Prostatic Hyperplasia with Natural Products: Perspective of New Pharmacological Agents. *Inflammation & Allergy - Drug Targets (Discontinued)* **2012**, *11*, 207-221, https://doi.org/10.2174/187152812800392715.
10. Debruyne, F.; Koch, G.; Boyle, P.; Da Silva, F.C.; Gillenwater, J.G.; Hamdy, F.C.; Perrin, P.; Teillac, P.; Vela-Navarrete, R.; Raynaud, J.P. Comparison of a phytotherapeutic agent (Permixon) with an alpha-blocker (Tamsulosin) in the treatment of benign prostatic hyperplasia: a 1-year randomized international study. *European urology* **2002**, *41*, 497-506; discussion 506-497.
11. Sökeland, J. Combined sabal and urtica extract compared with finasteride in men with benign prostatic hyperplasia: analysis of prostate volume and therapeutic outcome. *BJU International* **2000**, *86*, 439-442, https://doi.org/10.1046/j.1464-410x.2000.00776.x.
12. Jaiswal, Y.; Weber, D.; Yerke, A.; Xue, Y.; Lehman, D.; Williams, T.; Xiao, T.; Haddad, D.; Williams, L. A substitute variety for agronomically and medicinally important Serenoa repens (*Saw palmetto*). *Scientific Reports* **2019**, *9*, https://doi.org/10.1038/s41598-019-41150-z.
13. McClure, M.W. An overview of holistic medicine and complementary and alternative medicine for the prevention and treatment of BPH, prostatitis, and prostate cancer. *World Journal of Urology* **2002**, *20*, 273-284, https://doi.org/10.1007/s00345-002-0292-1.
14. Pagano, E.; Laudato, M.; Griffo, M.; Capasso, R. Phytotherapy of Benign Prostatic Hyperplasia. A Minireview. *Phytotherapy Research* **2014**, *28*, 949-955, https://doi.org/10.1002/ptr.5084.
15. Governa, P.; Giachetti, D.; Biagi, M.; Manetti, F.; De Vico, L. Hypothesis on Serenoa repens (Bartram) small extract inhibition of prostatic 5α-reductase through an in silico approach on 5β-reductase x-ray structure. *Peer J.* **2016**, *22*, https://doi.org/10.7717/peerj.2698.
16. Mando, H.; Hassan, A.; Gharaghani, S. Novel and Predictive QSAR Model for Steroidal and Nonsteroidal 5α- Reductase Type II Inhibitors. *Curr Drug Discov Technol*. **2021**, *18*, 317-332, https://doi.org/10.2174/1570163817666200324170457.
17. Khantham, C.; Yooin, W.; Sringarm, K.; Sommano, S.R.; Jiranusornkul, S.; Carmona, F.D.; Nimlamool, W.; Jantrawut, P.; Rachtanapun, P.; Ruksiriwanich, W. Effects on Steroid 5-Alpha Reductase Gene Expression of Thai Rice Bran Extracts and Molecular Dynamics Study on SRD5A2. *Biology* **2021**, *10*, https://doi.org/10.3390/biology10040319.
18. Mitsunari, K.; Miyata, Y.; Matsuo, T.; Mukae, Y.; Otsubo, A.; Harada, J.; Kondo, T.; Matsuda, T.; Ohba, K.; Sakai, H. Pharmacological Effects and Potential Clinical Usefulness of Polyphenols in Benign Prostatic Hyperplasia. *Molecules* **2021**, *26*, https://doi.org/10.3390/molecules26020450.
19. Han, H.Y.; Shan, S.; Zhang, X.; Wang, N.L.; Lu, X.P.; Yao, X.S. Down-regulation of prostate specific antigen in LNCaP cells by flavonoids from the pollen of Brassica napus L. *Phytomedicine* **2007**, *14*, 338-343, https://doi.org/10.1016/j.phymed.2006.09.005.
20. Bektic, J.; Guggenberger, R.; Spengler, B.; Christoffel, V.; Pelzer, A.; Berger, A.P.; Ramoner, R.; Bartsch, G.; Klocker, H. The flavonoid apigenin inhibits the proliferation of prostatic stromal cells via the MAPK-pathway and cell-cycle arrest in G1/S. *Maturitas* **2006**, *55*, S37-S46, https://doi.org/10.1016/j.maturitas.2006.06.015.
21. Chen, M.Y.; Yan, S.C.; Yin, C.P.; Ye, L.; Zhang, M.K.; Yang, J.; Liu, J.H. Red clover isoflavones inhibit the proliferation and promote the apoptosis of benign prostatic hyperplasia stromal cells. *Zhonghua Nan Ke Xue*, **2010**, *16*, 34-39.
22. Hiipakka, R.A.; Zhang, H.-Z.; Dai, W.; Dai, Q.; Liao, S. Structure–activity relationships for inhibition of human 5α-reductases by polyphenols. *Biochemical Pharmacology* **2002**, *63*, 1165-1176, https://doi.org/10.1016/s0006-2952(02)00848-1.
23. Ghidoli, M.; Colombo, F.; Sangiorgio, S.; Landoni, M.; Giupponi, L.; Nielsen, E.; Pilu, R. Food Containing Bioactive Flavonoids and Other Phenolic or Sulfur Phytochemicals With Antiviral Effect: Can We Design a Promising Diet Against COVID-19? *Frontiers in Nutrition* **2021**, *8*, https://doi.org/10.3389/fnut.2021.661331.
24. Hiremath, S.; Kumar, H.D.V.; Nandan, M.; Mantesh, M.; Shankarappa, K.S.; Venkataravanappa, V.; Basha, C.R.J.; Reddy, C.N.L. In silico docking analysis revealed the potential of phytochemicals present in Phyllanthus amarus and Andrographis paniculata, used in Ayurveda medicine in inhibiting SARS-CoV-2. *3 Biotech* **2021**, *11*, https://doi.org/10.1007/s13205-020-02578-7.
25. Moussa, N.; Hassan, A.; Singab, A. Quality control of herbal medicines used for arthritis: Identification and Quantification of COX Inhibitors by HPLC, GC-MS, LC-MS-MS, GC-FID. *Acta Poloniae Pharmaceutica - Drug Research* **2021**, *78*, 157-167, https://doi.org/10.32383/appdr/134001.
26. Gong, G.; Guan, Y.-Y.; Zhang, Z.-L.; Rahman, K.; Wang, S.-J.; Zhou, S.; Luan, X.; Zhang, H. Isorhamnetin: A review of pharmacological effects. *Biomedicine & Pharmacotherapy* **2020**, *128*, https://doi.org/10.1016/j.biopha.2020.110301.

27. Jayadeepa, R.M.; Sharma, S. Computational Models for 5αR Inhibitors for Treatment of Prostate Cancer: Review of Previous Works and Screening of Natural Inhibitors of 5αR2. *Current computer-aided drug design* **2011**, *7*, 231-237, https://doi.org/10.2174/157340911798260368.
28. Xiao, Q.; Wang, L.; Supekar, S.; Shen, T.; Liu, H.; Ye, F.; Huang, J.; Fan, H.; Wei, Z.; Zhang, C. Structure of human steroid 5α-reductase 2 with the anti-androgen drug finasteride. *Nature Communications* **2020**, *11*, https://doi.org/10.1038/s41467-020-19249-z.
29. Maestro 9.9. Schrödinger, LLC.; New York: **2019**. https://www.schrodinger.com/maestro. (Accessed on 15 September 2021).
30. Syed Sauban Ghani, S.S. A comprehensive review of database resources in chemistry. *Eclética Química Journal* **2020,** *45*, 57-68**,** https://doi.org/10.26850/1678-4618eqj.v45.3.2020.p57-68.
31. O'Boyle, N.M.; Banck, M.; James, C.A.; *et al.* Open Babel: An open chemical toolbox. *J Cheminform* **2011**, *3*, 33. https://doi.org/10.1186/1758-2946-3-33.
32. Harder, E.; Damm, W.; Maple, J.; Wu, C.; Reboul, M.; Xiang, J.Y. OPLS3: a force field providing broad coverage of drug-like small molecules and proteins. *J. Chem. Theor. Comput.* **2016**, *12*, 281–296, https://doi.org/10.1021/acs.jctc.5b00864.
33. Storer, J.W.; Giesen, D.J.; Cramer, C.J.; Truhlar, D.G. Class IV charge models: a new semi empirical approach in quantum chemistry. *J. Comput. Aided Mol. Des* **1995**, *9*, 87–110, https://doi.org/10.1007/BF00117280.
34. Madhavi, S.G.; Adzhigirey, M.; Day, T.; Annabhimoju, R.; Sherman, W. Protein and ligand preparation: parameters, protocols, and influence on virtual screening enrichments, *J. Comput. Aided Mol. Des*. **2013**, *27*, 221–234, https://doi.org/10.1007/s10822-013-9644-8.
35. Xiao, Q.; Wang, L.; Supekar, S.; Shen, T.; Liu, H.; Ye, F.; Huang, J.; Fan, H.; Wei, Z.; Zhang, C. Structure of human steroid 5α-reductase 2 with the anti-androgen drug finasteride. *Nature Communications* **2020**, *11*, https://doi.org/10.1038/s41467-020-19249-z.
36. Friesner, R.A.; Banks, J.L.; Murphy, R.B.; Halgren, T.A.; Klicic, J.J.; Mainz, D.T.; Repasky, M.P.; Knoll, E.H.; Shelley, M.; Perry, J.K.; Shaw, D.E.; Francis, P.; Shenkin, P.S. Glide: A New Approach for Rapid, Accurate Docking and Scoring. 1. Method and Assessment of Docking Accuracy. *Journal of Medicinal Chemistry* **2004**, *47*, 1739-1749, https://doi.org/10.1021/jm0306430.
37. Friesner, R.A.; Murphy, R.B.; Repasky, M.P.; Frye, L.L.; Greenwood, J.R.; Halgren, T.A.; Sanschagrin, P.C.; Mainz, D.T. Extra Precision Glide: Docking and Scoring Incorporating a Model of Hydrophobic Enclosure for Protein−Ligand Complexes. *Journal of Medicinal Chemistry* **2006**, *49*, 6177-6196, https://doi.org/10.1021/jm051256o.
38. Chen, G.; Li, X.; Saleri, F.; Guo, M. Analysis of Flavonoids in Rhamnus davurica and Its Anti-proliferative Activities. *Molecules* **2016,** *21*, https://doi.org/10.3390/molecules21101275.
39. Abdul Latiff, N.; Suan, C.L.; Sarmidi, M.R.; Ware, I.; Abdul Rashid, S.N.S.; Yahayu, M. Liquid chromatography tandem mass spectrometry for the detection and validation of quercetin-3-o-rutinoside and myricetin from fractionated Labisia pumilavar. *Alata. Malaysian J. Anal. Sci* **2018**, *22*, 817-827, https://doi.org/10.17576/mjas-2018-2205-09.
40. Yuan, L.; Ding, M.; Ma, J.; Xu, J.; Wu, X.; Feng, J.; Zhou, X. Determination of finasteride in human plasma by liquid chromatography–electrospray ionization tandem mass spectrometry with flow rate gradient. *Eur J Drug Metab Pharmacokinet* **2010**, *35*, 137–146, https://doi.org/10.1007/s13318-010-0013-x.
41. Panlin, Li.; Weiwei, Su.; Chengshi, Xie.; Zeng, X.; Peng, W.; Liu, M. Rapid Identification and Simultaneous Quantification of Multiple Constituents in Nao-Shuan-Tong Capsule by Ultra-Fast Liquid Chromatography/Diode-Array Detector/Quadrupole Time-of-Flight Tandem Mass Spectrometry. *J. Chromatogr. Sci.* **2015**, *53*, 886–897, https://doi.org/10.1093/chromsci/bmu137.
42. Li, A.; Hou, X.; Wei, Y. Fast screening of flavonoids from switchgrass and Mikania micrantha by liquid chromatography hybrid-ion trap time-of-flight mass spectrometry. *Anal. Methods* **2018**, *10*, 109–122, https://doi.org/10.1039/C7AY02103H.
43. Chen, Y.; Yu, H.; Wu, H.; Pan, Y.; Wang, K.; Jin, Y.; Zhang, C. Characterization and Quantification by LC-MS/MS of the Chemical Components of the Heating Products of the Flavonoids Extract in Pollen Typhae for Transformation Rule Exploration. *Molecules* **2015**, *20*, 18352–18366, https://doi.org/10.3390/molecules201018352.
44. Lin, Y.; Wu, B.; Li, Z.; Hong, T.; Chen, M.; Tan, Y.; Huang, C. Metabolite Identification of Myricetin in Rats Using HPLC Coupled with ESI-MS. *Chromatographia* **2012**, *75*, 655–660, https://doi.org/10.1007/s10337-012-2239-z.
45. Ben Said, R.; Hamed, A.I.; Mahalel, U.A.; Al-Ayed, A.S.; Kowalczyk, M.; Moldoch, J.; Oleszek, W.; Stochmal, A. Tentative Characterization of Polyphenolic Compounds in the Male Flowers of Phoenix dactylifera by Liquid Chromatography Coupled with Mass Spectrometry and DFT. *International Journal of Molecular Sciences* **2017**, *18*, https://doi.org/10.3390/ijms18030512.
46. Chen, Y. Characterization and Quantification by LC-MS/MS of the Chemical Components of the Heating Products of the Flavonoids Extract in Pollen Typhae for Transformation Rule Exploration. *Molecules* **2015**, *20*, 18352-18366, https://doi.org/10.3390/molecules201018352.

47. Wang, X.; Qian, Y.; Li, X.; Jia, X.; Yan, Z.; Han, M.; Qiao, M.; Ma, X.; Chu, Y.; Zhou, S.; Yang, W. Rapid determination of rosmarinic acid and its two bioactive metabolites in the plasma of rats by LC–MS/MS and application to a pharmacokinetics study. *Biomed. Chromatogr*. **2021**, *35*, https://doi.org/10.1002/bmc.4984.
48. Simirgiotis, M.J.; Benites, J.; Areche, C.; Sepúlveda, B. Antioxidant Capacities and Analysis of Phenolic Compounds in Three Endemic Nolana Species by HPLC-PDA-ESI-MS. *Molecules* **2015**, *20*, 11490-507, https://doi.org/10.3390/molecules200611490.
49. Chen, G.; Li, X.; Saleri, F.; Guo, M. Analysis of Flavonoids in Rhamnus davurica and Its Anti-proliferative Activities. *Molecules* **2016**, *21*, https://doi.org/10.3390/molecules21101275.
50. Tatar, G.; Salmanli, M.; Dogru, Y.; Tuzuner, T. Evaluation of the effects of chlorhexidine and several flavonoids as antiviral purposes on SARS-CoV-2 main protease: molecular docking, molecular dynamics simulation studies. *Journal of Biomolecular Structure and Dynamics* **2021**, 1-10, https://doi.org/10.1080/07391102.2021.1900919.
51. Foddai, M.; Maldini, M.; Addis, R.; Petretto, G.L.; Chessa, M.; Pintore, G. Profiling of the Bioactive Compounds in Flowers, Leaves and Roots of Vinca sardoa. *Natural Product Communications* **2017**, *12*, https://doi.org/10.1177/1934578X1701200625.
52. Reed, K.A. *Identification of Phenolic Compounds from Peanut Skin using HPLC-MS.* December 7, **2009** Blacksburg, Virginia.
53. Sun, J.; Liang, F.; Bin, Y.; Li, P.; Duan, C. Screening Non-colored Phenolics in Red Wines using Liquid Chromatography/Ultraviolet and Mass Spectrometry/Mass Spectrometry Libraries. *Molecules* **2007**, *12*, 679-693, https://doi.org/10.3390/12030679.
54. Xu, F.; Liu, Y.; Zhang, Z.; Yang, C.; Tian, Y. Quasi-MSn identification of flavanone 7-glycoside isomers in Da Chengqi Tang by high performance liquid chromatography-tandem mass spectrometry. *Chinese Medicine* **2009**, *4*, https://doi.org/10.1186/1749-8546-4-15.
55. Jung, U.J.; Kim, H.J.; Lee, J.S.; Lee, M.K.; Kim, H.O.; Park, E.J.; Kim, H.K.; Jeong, T.S.; Choi, M.S. Naringin supplementation lowers plasma lipids and enhances erythrocyte antioxidant enzyme activities in hypercholesterolemic subjects. *Clinical Nutrition* **2003**, *22*, 561-568, https://doi.org/10.1016/s0261-5614(03)00059-1.
56. Renugadevi, J.; Prabu, S.M. Naringenin protects against cadmium-induced oxidative renal dysfunction in rats. *Toxicology* **2009**, *256*, 128-134, https://doi.org/10.1016/j.tox.2008.11.012.
57. Den Hartogh, D.J.; Tsiani, E. Antidiabetic Properties of Naringenin: A Citrus Fruit Polyphenol. *Biomolecules* **2019**, *9*, 1–21, https://doi.org/10.3390/biom9030099.
58. Esposito, E.X.; Baran, K.; Kelly, K.; Madura, J.D. Docking of sulfonamides to carbonic anhydrase II and IV11Color Plate 1, Color Plate 2, Color Plate 3, Color Plate 4 for this article are on pages 307–308. *Journal of Molecular Graphics and Modelling* **2000**, *18*, 283-289, https://doi.org/10.1016/s1093-3263(00)00040-1.
59. Lucas, X.; Bauzá, A.; Frontera, A.; Quiñonero, D. A thorough anion–π interaction study in biomolecules: on the importance of cooperativity effects. *Chemical Science* **2016**, *7*, 1038-1050, https://doi.org/10.1039/C5SC01386K.
60. Ferrari, L.; Stucchi, R.; Konstantoulea, K.; van de Kamp, G.; Kos, R.; Geerts, W.J.C.; van Bezouwen, L.S.; Förster, F.G.; Altelaar, M.; Hoogenraad, C.C.; Rüdiger, S.G.D. Arginine π-stacking drives binding to fibrils of the Alzheimer protein Tau. *Nature Communications* **2020**, *11*, https://doi.org/10.1038/s41467-019-13745-7.
61. Bender, O.; Atalay, A. *Polyphenol chlorogenic acid, antioxidant profile, and breast cancer. Cancer Oxidative Stress and Dietary Antioxidants* 2nd ed.; Victor, R.; Patel, V.B. Academic Press Elsevier: **2021**; pp. 311-321, https://doi.org/10.1016/B978-0-12-819547-5.00028-6.
62. Kurczab, R.; Śliwa, P.; Rataj, K.; Kafel, R.; Bojarski, A.J. Salt Bridge in Ligand–Protein Complexes—Systematic Theoretical and Statistical Investigations. *J. Chem. Inf. Model*. **2018**, *58*, 2224–2238, https://doi.org/10.1021/acs.jcim.8b00266.